DOI: 10.1002/chem.200701892

Synthesis and Complexation of Multiarmed Cycloveratrylene-Type Ligands: Observation of the "Boat" and "Distorted-Cup" Conformations of a Cyclotetraveratrylene Derivative

Christopher J. Sumby,*[a, b] Keith C. Gordon,[c] Tim J. Walsh,[c] and Michaele J. Hardie*[a]

Abstract: Investigations of a previously reported ligand, hexakis(2-pyridylmethyl)cyclotricatechylene (**1**), and a new tetrameric bridging ligand, octakis(2-pyridylmethyl)cyclotetracatechylene (**2**), the latter constructed on a larger cyclotetraveratrylene (CTTV) scaffold, are described. Variable-temperature NMR studies support a "sofa" conformation for **2**, akin to studies on the parent compound. The coordination chemistry of **2** and its smaller trimeric homologue have also been investigated with silver(I), copper(II) and palladium(II) salts. An unexpected chelating mode was observed for **1** in the structure of DMF⊂$[Pd_3Cl_6(\mathbf{1})]$·DMF, whereby the palladium cations bridge two veratrole subunits rather than chelating within a single subunit. In the structure of $[Ag_4(\mathbf{2})][Co(C_2B_9H_{11})_2]_4$·2.8 CH_3CN·H_2O, ligand **2** adopts a "boat" conformation, whereas in $[Pd_4Cl_8(\mathbf{2})]$·4 H_2O, ^{1}H NMR spectroscopic studies and calculations indicate that the ligand is present in a previously unobserved "distorted-cup" conformation. This conformation was calculated to be approximately 90 kJ mol^{-1} lower in energy than the alternative "sofa" conformation. Thus, coordination-induced conformational control over CTTV derivatives offers new routes to exploit the host–guest chemistry of these compounds.

Keywords: bridging ligands · conformational isomerism · coordination modes · host–guest systems · supramolecular chemistry

Introduction

The conformational mobility of the cyclic tetramer of veratrole, cyclotetraveratrylene (CTTV), has been the subject of some attention[1–6] since its structure, and that of the smaller trimer cyclotriveratrylene (CTV), was firmly established.[1,2,7] Unlike CTV, which generally adopts a rigid bowl-shaped conformation,[8,9] CTTV and its derivatives have been demonstrated to undergo pseudo-rotations of equivalent conformations at room temperature.[2,6] Two conformations have been deliberated: a C_{2h} symmetry "sofa" conformation and a C_{2v} symmetry "boat" conformation. Dynamic NMR spectroscpic investigations of CTTV and the related demethylated compound, cyclotetracatechylene (CTTC), have determined that the solution species are consistent with a sofa conformation. This converts through fast pseudo-rotations about the sp^3-sp^2-sp^2-sp^3 bonds,[2,6] and not through a postulated C_{4v} symmetric "crown" conformation.[1,2] This latter crown is postulated to be unstable due to steric clashes between the aromatic rings.[1,2] However, for host–guest studies, this unstable crown conformation is highly desirable, as it allows for complexation of large spherical guests, such as fullerenes, akin to reported ball-and-socket-type complexes with CTV.[10] One report describes an attempt to stabilise the crown conformation through chemical modification.[6]

We have been investigating the use of chelating derivatives of CTV functionalised with pyridyl transition-metal binding moieties, to prepare coordination polymers displaying porosity and unusual host–guest phenomena.[11] To this end, we have synthesised and reported the hexadentate three-connecting ligand, hexakis(2-pyridylmethyl)cyclotricatechylene (**1**).[12] The related veratrole tetramer CTTV

[a] Dr. C. J. Sumby, Dr. M. J. Hardie
School of Chemistry, University of Leeds
Woodhouse Lane, Leeds LS2 9JT (UK)
Fax: (+44) 113-343-6565
E-mail: christopher.sumby@adelaide.edu.au
m.j.hardie@leeds.ac.uk

[b] Dr. C. J. Sumby
Present address: School of Chemistry & Physics
The University of Adelaide
North Terrace, Adelaide, SA 5025 (Australia)
Fax: (+61) 8-8303-4358

[c] Prof. K. C. Gordon, T. J. Walsh
Department of Chemistry, University of Otago
Dunedin 9001 (New Zealand)

Supporting information for this article is available on the WWW under http://www.chemeurj.org/ or from the author.

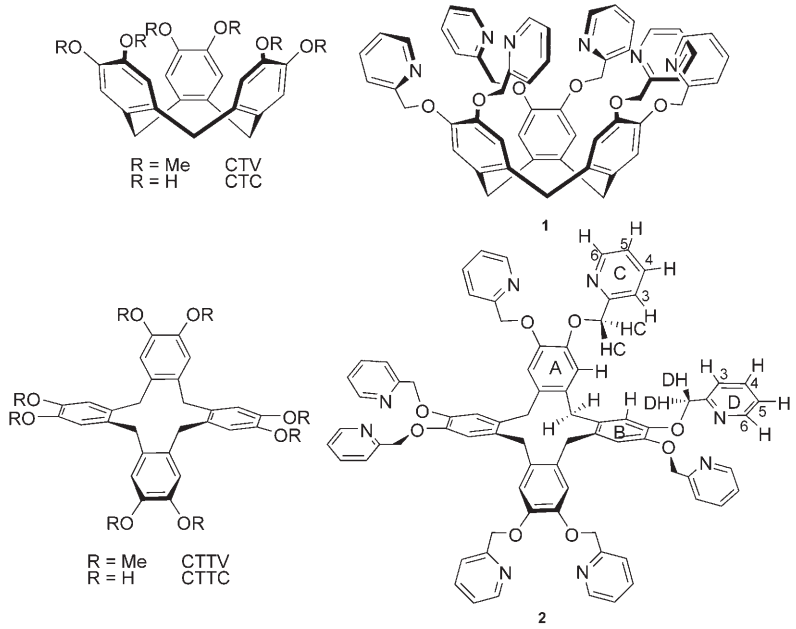

caught our attention as a route to a four-connecting chelating ligand with a useful three-dimensional displacement of the donor groups.[4,5,13] Thus, the ligand octakis(2-pyridylmethyl)cyclotetracatechylene (**2**) was prepared to extend this approach.

While there are a few known examples of discrete metal complexes of CTV derivatives,[14] none are reported for derivatives of CTTV. The two ligands display identical N_2O_2 coordination sites potentially suitable for the chelation of transition-metal atoms. Ligand **1** displays three such pockets, whereas **2** has four identical coordination sites, which suggests that these ligands could serve as bridging ligands for three and four transition metals, respectively, in a manner suitable for the formation of discrete complexes or coordination polymers. Multidentate ligands of this nature, with six and eight donor arms, have previously been investigated with simple planar arene scaffolds.[15,16] Ligands with two-atom linker groups between the terminal heterocycle and the central arene ring that contains at least one sulfur or oxygen atom, such as **1** and **2**, have been described.[16–19] Most of the reported examples have benzyl or picolinyl cores with the heteroatom directly bonded to the terminal heterocycle.[16,18,19] Metal complexes of these ligands typically show chelation to transition-metal atoms by the *ortho*-positioned heterocyclic donor groups in a manner that has led to the formation of either discrete coordination complexes or extended coordination polymers. Notably, the sulfur and oxygen atoms adjacent to the heterocycle in the linker groups are involved in coordinating to the metal atom.[16,19]

Herein, we describe the synthesis of the tetrameric ligand **2**, and variable-temperature (VT) NMR investigations of this new compound. Discrete coordination complexes of the two pyridyl ligands **1** and **2** are reported for silver(I), copper(II) and palladium(II) salts. In addition to observing an unexpected chelating mode for **1**, coordination-induced conformational control over ligand **2** was observed for silver(I) and palladium(II) complexes.

Results and Discussion

Synthesis of 2: The synthetic procedure for the preparation of **1** was described in a previous publication.[12] By using the protocols previously described, the larger octadentate ligand **2** was prepared in relatively low yield (Scheme 1). Carrying out the alkylation reaction of CTTC in acetone effected the transformation to **2** in a low 17% yield,

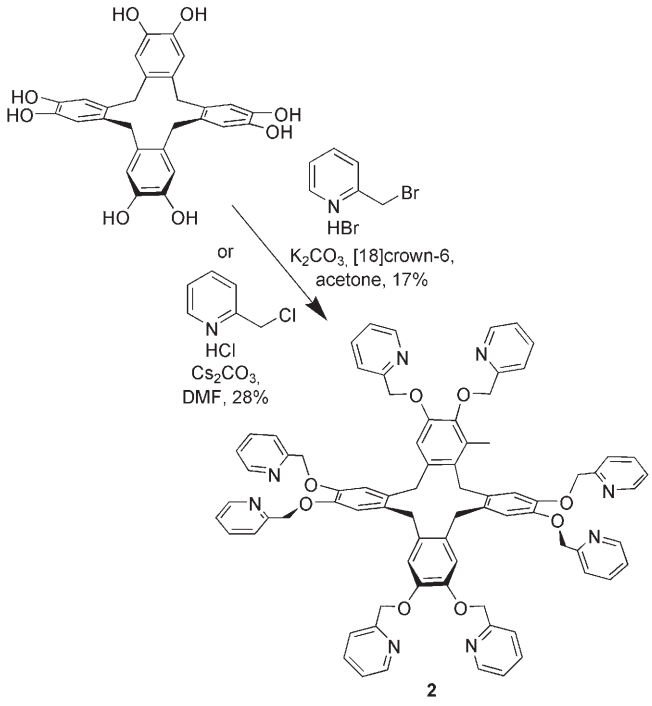

Scheme 1. Two variations on the synthetic approach to the synthesis of compound **2**.

whereas a slight improvement (28%) was obtained by performing the reaction in DMF with a more soluble base, caesium carbonate. Although these yields are modest, they are workable considering that a total of eight alkylation reactions is required to form each molecule of **2**.

The new ligand **2** was characterised by mass spectrometry, elemental analysis and NMR spectroscopy. ^{1}H NMR spectroscopy of **2** highlighted the distinctive feature of CTTV

chemistry that distinguishes it from the chemistry of the trimer; namely, the slow room-temperature interconversion (on the NMR timescale) of the conformation of the tetrameric core. The ^{1}H NMR spectrum of **2** at room temperature (303 K) consists of several broad peaks for the benzyl protons, the aryl ring protons and the methyl protons, indicative of this slow conversion (Figure 1a). The pyridyl proton signals are slightly less broadened by comparison, as these are more remote from the central cyclododecatetraene ring. The room-temperature spectrum of **2** is consistent with that of the parent compound, CTTC, which exists in four equivalent "sofa" conformers.[6] Recording the ^{1}H NMR spectrum of **2** at a higher temperature (333 K) leads to a sharpening of the spectrum to give one set of signals consistent with rapid conversion (on the NMR timescale) of these sofa conformations (Figure 1a). Cooling the sample down to 233 K freezes out this dynamic process and gives a spectrum that is consistent with a C_{2h} sofa conformer (Figure 1a). This spectrum consists of two sets of signals for the chemically non-equivalent pyridyl rings, two singlets for the two chemically non-equivalent aryl protons and a splitting of the signal for the benzenoid protons of the base of the CTTV ring. The remaining two signals arise from the sp^3–CH_2 linker on the upper rim of the CTTV bowl; one signal appears as a singlet, whereas the other appears as a doublet of doublets. The VT solution behaviour of the new ligand **2** is consistent with that observed for the parent compounds CTTV[1,2] and CTTC,[6] and other related compounds.[12]

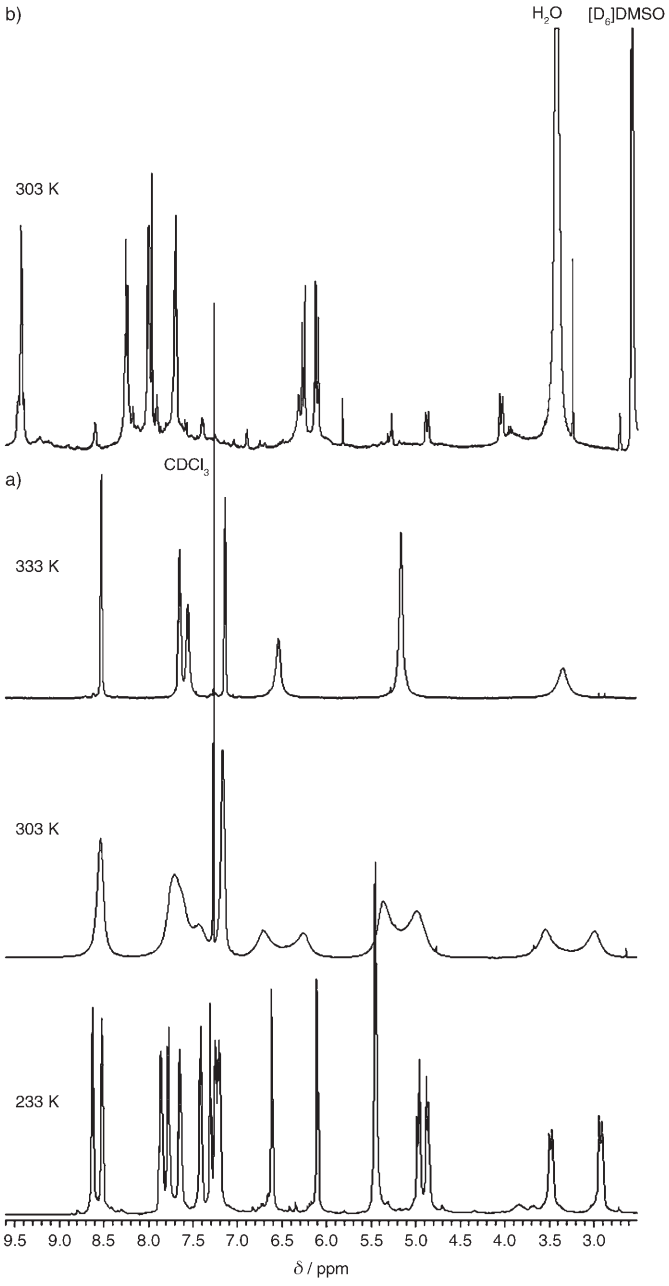

Figure 1. a) VT ^{1}H NMR spectra of ligand **2** in $CDCl_3$ at 233, 303 and 333 K and b) the ^{1}H NMR spectrum of $[Pd_4Cl_8(\mathbf{2})]\cdot 4H_2O$ in $[D_6]$DMSO at 303 K.

Complexes of 1: To examine the coordination chemistry of **1**, the ligand was reacted with a number of transition-metal salts including silver(I) cobalticarborane, copper(II) chloride, copper(II) bromide, palladium(II) chloride and palladium(II) trifluoroacetate (Scheme 2). A trinuclear silver

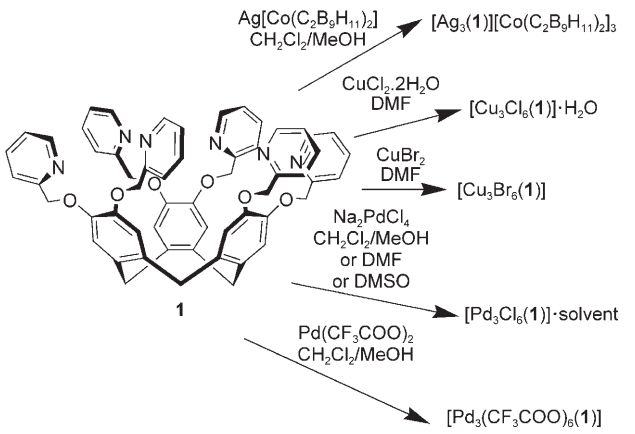

Scheme 2. Complexes formed with ligand **1** and routes to prepare these complexes.

complex, $[Ag_3(\mathbf{1})][Co(C_2B_9H_{11})_2]_3$, was prepared by layering a solution of $Ag[Co(C_2B_9H_{11})_2]$ in methanol over a dichloromethane solution of the ligand. This gave a yellow solid that was characterised by combustion analysis, IR spectroscopy (shifts of several bands) and ^{1}H NMR spectroscopy. The trinuclear silver complex was also observed in solution by electrospray mass spectrometry (ESMS). The complex displays C_3 symmetry in solution and a number of coordination-induced shifts ($CIS = \delta_{complex} - \delta_{ligand}$) confirm coordination to three silver centres (see the Supporting Information). Similarly, trinuclear copper(II) complexes of **1** were prepared from copper(II) chloride and copper(II) bromide, which analysed with the compositions $[Cu_3Cl_6(\mathbf{1})]\cdot H_2O$ and $[Cu_3Br_6(\mathbf{1})]$, respectively. Despite extensive efforts, none of

the three complexes could be recrystallised to provide crystals suitable for X-ray crystallographic studies.

In contrast, reaction of **1** with two palladium salts yielded single crystals. Reaction of a methanol solution of $Pd(CF_3COO)_2$ with a dichloromethane solution of the ligand yielded small yellow crystals of $[Pd_3(CF_3COO)_6(\mathbf{1})]$ after several days. Unfortunately these crystals were extremely sensitive to solvent loss; removal from the mother liquor resulted in almost instantaneous loss of crystallinity. Various attempts to mount the crystals in sealed capillaries were unsuccessful. Reaction of the ligand with $Na_2[PdCl_4]$ however, yielded crystals of $[Pd_3Cl_6(\mathbf{1})]$·solvent that were found to be more stable. The complex was obtained by a number of routes, as outlined in Scheme 2. Small yellow block-shaped crystals of DMF⊂$[Pd_3Cl_6(\mathbf{1})]$·DMF suitable for X-ray crystallography were obtained from the reaction of $Na_2[PdCl_4]$ and **1** with DMF as the solvent, in a capped vial at 100 °C. The filtrate of this reaction also yielded small petal-shaped crystals in a minuscule yield of $(DMF)_{0.5}\subset[Pd_2Cl_4(\mathbf{1})]\cdot 2H_2O$ by vapour diffusion of ethanol, the structure of which was also elucidated. A DMSO solvate, $[Pd_3Cl_6(\mathbf{1})]\cdot 2$DMSO, could also be obtained by carrying out the reaction under the same conditions in DMSO solvent. The palladium chloride complexes of **1** proved to be very insoluble in common laboratory solvents, and thus no characterisation was undertaken in solution.

Structure of DMF⊂$[Pd_3Cl_6(1)]$·DMF: A C_3-symmetric trinuclear palladium chloride complex was proposed on the basis of combustion analysis. This composition was confirmed by X-ray crystallography that also revealed an unexpected twist in the mode of coordination—instead of chelating to a palladium atom within each veratrole unit, the pyridyl groups are oriented to place the palladium centres between two veratrole groups. The complex DMF⊂$[Pd_3Cl_6(\mathbf{1})]$·DMF crystallised in the monoclinic space group $P2_1/m$ with one half of the complex (located on the mirror plane) and two DMF molecules (also located on the mirror plane) in the asymmetric unit (Figure 2). Two perspective views of the $[Pd_3Cl_6(\mathbf{1})]$ complex are shown in Figure 3, highlighting the threefold complexation and bowl-shaped nature of the complex.

The palladium centres both have a square-planar geometry with bond lengths typical of such a coordination environment. In the complex, ligand **1** has much the same overall bowl conformation as it possesses when crystallised from methanol,[12] but the pyridyl groups are oriented in the opposite direction. The palladium cations bridge between the veratrole groups rather than the expected binding mode. This may arise because the ligand possesses a pocket more suited to binding a square-planar palladium centre in this conformation; the distance between the coordinating nitrogen atoms is between 4.07 and 4.09 Å, whereas the distance between the pyridyl nitrogen atoms within a veratrole ring in the crystal structure of **1** is 4.44 Å.[12] In the palladium complex, the distance between the C3 atoms of the pyridyl rings within a veratrole ring is between 4.91 and 5.56 Å. In the conformation observed in the crystal structure, the CH_2O linkages are almost maintained in the plane of the veratrole rings to which they are attached (torsion angles for C-C-O-CH_2 between 12.2 and 29.5°).

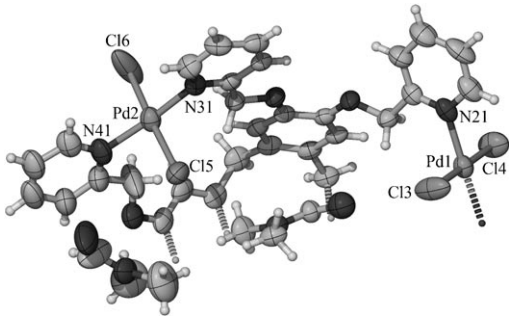

Figure 2. ORTEP representation (at the 50% probability level) of the asymmetric unit of the trinuclear palladium complex DMF⊂$[Pd_3Cl_6(\mathbf{1})]$·DMF, with selected atomic labelling. The symmetry-generated hydrogen atoms of the encapsulated DMF molecule are shown for clarity. Selected bond lengths [Å] and angles [°]: Pd1–N21 2.044(8), Pd1–Cl4 2.285(3), Pd1–Cl3 2.294(3), Pd2–N31 2.027(7), Pd2–N41 2.047(8), Pd2–Cl6 2.275(3), Pd2–Cl5 2.307(3); N21-Pd1-N21 176.6(4), N21-Pd1-Cl4 91.00(17), N21-Pd1-Cl3 89.01(17), Cl4-Pd1-Cl3 179.6(2), N31-Pd2-N41 172.8(3), N31-Pd2-Cl6 89.4(2), N41-Pd2-Cl6 90.1(2), N31-Pd2-Cl5 89.71(19), N41-Pd2-Cl5 91.3(2), Cl6-Pd2-Cl5 175.70(17).

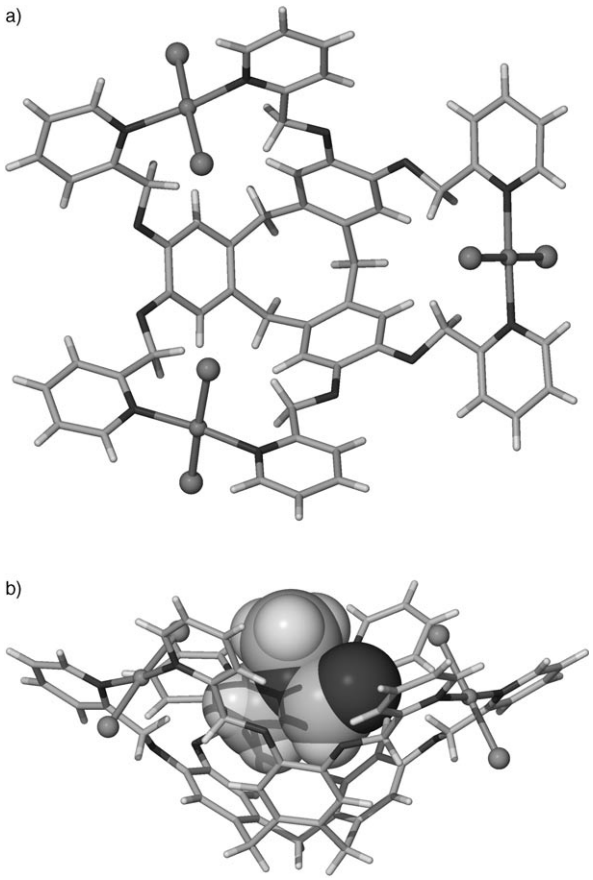

Figure 3. Two perspective views of the trinuclear complex DMF⊂$[Pd_3Cl_6(\mathbf{1})]$·DMF from a) above the central CTV core and b) the side with the guest DMF molecule shown in a space-filling representation.

Interestingly, the trinuclear palladium complex does not crystallise with C_3 symmetry; instead, a mirror plane running through Pd1, C1 and the opposite veratrole ring bisects the molecule. This unexpected symmetry is represented by the separations between the centroids of the veratrole rings. Along the mirror plane, the centroid–centroid distance is 4.82 Å, wheras across the mirror plane the corresponding distance is 4.38 Å. This finding indicates that the CTV base of the ligand may be pinched to provide a better fit to the included DMF guest molecule in the solid state. This DMF molecule is also located along the mirror plane with the formyl hydrogen atom and a methyl group placed within the cavity of the host ligand. The body centre of the DMF molecule is located 5.14 Å above the $-(CH_2)_3-$ centroid of the CTV base, which indicates that the guest perches above the cavity. No significant interactions (CH···π interactions) are obvious as none of the hydrogen atoms of the guest are directed toward any of the veratrole rings.

Within the extended structure of DMF⊂[Pd_3Cl_6(**1**)]·DMF, the individual host–guest species are arranged into weakly hydrogen-bonded one-dimensional tapes (along the *b* axis of the unit cell). Each complex forms two long C–H···O hydrogen bonds (d = 2.67 Å, D = 3.59 Å) to the guest DMF molecule of two adjacent host–guest species. In the resulting tapes the complexes are arranged in alternating bowl-up-bowl-down orientations that give a zigzag appearance to the hydrogen-bonded chains. The tapes are then assembled into layers in the *bc* plane with edge-to-face and face-to-face π-stacking interactions apparent between the tapes. Packing of these layers within the crystal completes the crystal packing.

During attempts to obtain the above structure, crystals of a dinuclear palladium complex were obtained and the structure determined by X-ray crystallography. Again, the unexpected coordination mode is observed for the ligand. There are two crystallographically distinct dinuclear complexes in the structure and both show significant disorder of their unbound pyridyl groups. As before, the dinuclear complex acts as a host for a DMF guest molecule that is orientated along a mirror plane within the complex, although this guest could only be well resolved for one of the two complexes (Figure 4). The same contraction of the CTV cavity is observed across the mirror plane with the vacant coordination site heavily disordered. This may indicate that the binding of a third palladium centre is more difficult than the first two, and that the pinched conformation of the complex may result from binding the guest DMF molecule.

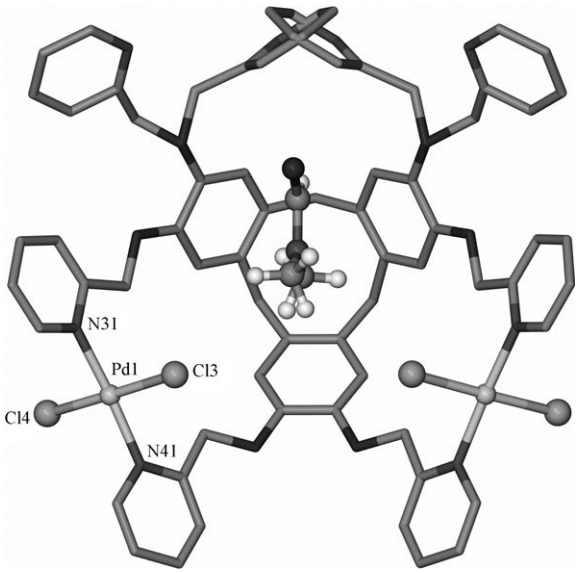

Figure 4. One of the two crystallographically independent dimeric complexes from the X-ray structure of $(DMF)_{0.5}$⊂[Pd_2Cl_4(**1**)]·2H_2O, with selected atomic labelling. Selected bond lengths [Å] and angles [°]: Pd1–N31 2.012(10), Pd1–Cl4 2.281(3), Pd1–Cl3 2.302(3); N31-Pd1-N41 174.4(3), N31-Pd1-Cl4 88.9(3), N41-Pd1-Cl4 91.5(3), N31-Pd1-Cl3 90.7(3), N41-Pd1-Cl3 89.1(3), Cl4-Pd1-Cl3 178.21(15).

Complexes of 2: Initial reactions of **2** with silver salts, in particular $Ag[Co(C_2B_9H_{11})_2]$, yielded microcrystalline powders. Slowing the rate of precipitation of the complex down sufficiently provided yellow crystals of [Ag_4(**2**)][$Co(C_2B_9H_{11})_2$]$_4$·2.8CH_3CN·H_2O that were suitable for X-ray crystallography. An ^{1}H NMR spectrum of the $[Ag_4(\mathbf{2})]^{4+}$ complex, which is not particularly soluble in common NMR solvents, indicates that the complex is labile and possibly conformationally mobile in solution, as indicated by very broad signals. ESMS showed no evidence for the molecular ion in solution. As shown in Scheme 3, a tetranuclear copper bromide complex of **2**, [Cu_4Br_8(**2**)], was also isolated and characterised by combustion analysis and IR spectroscopy (shifts in various absorption bands).

The most interesting and significant result observed for ligand **2** occurred upon reaction of this ligand with four

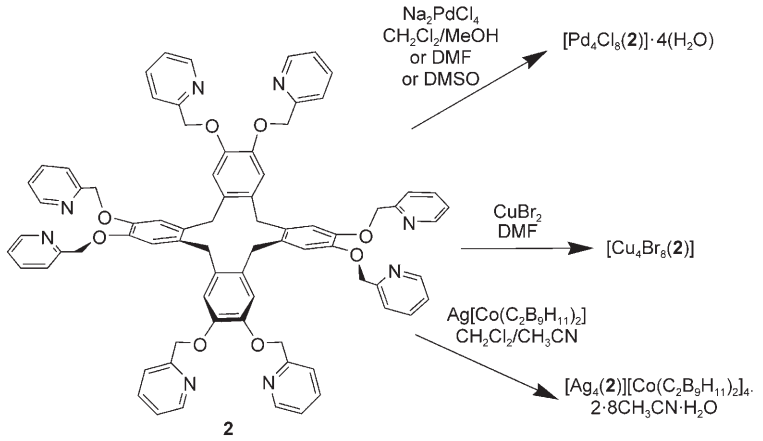

Scheme 3. Complexes reported for ligand **2**.

equivalents of $Na_2[PdCl_4]$. Undertaking the reaction in a variety of solvents (CH_2Cl_2/CH_3OH, DMF or DMSO) led to the isolation of a tetranuclear complex, $[Pd_4Cl_8(\mathbf{2})]$, that was characterised by combustion analysis and IR spectroscopy. The stoichiometry of this complex in solution was confirmed by ESMS, which showed a peak at m/z: 927.5, consistent with the doubly charged tetranuclear complex $[Pd_4Cl_6(\mathbf{2})]^{2+}$.

The ^{1}H NMR spectrum of $[Pd_4Cl_8(\mathbf{2})]$ at room temperature (303 K) in $[D_6]$DMSO shows several interesting and unexpected features. The most notable and significant of these features are the sharpness of the spectrum and the observed high symmetry of the compound (Figure 1b). Whereas direct comparisons of chemical shifts are not possible as the ligand and palladium complex have incompatible solubilities in common NMR spectroscopic solvents, the $[Pd_4Cl_8(\mathbf{2})]$ complex has a much sharper and simpler spectrum than the equivalent ^{1}H NMR spectrum of **2** at 303 K. A number of general downfield shifts for various signals are observed in the spectrum of $[Pd_4Cl_8(\mathbf{2})]$ that are consistent with coordination. The significant downfield shift of the pyridyl H6 ($\delta =$ 9.42 versus 8.55 ppm) supports the coordination of the palladium centre. Most significantly, the methylene $-(CH_2)_4-$ signals of the base of the CTTC core sharpen into two distinct doublets with one of the doublets moving significantly downfield. The $-(CH_2)_4-$ signals adopt the appearance and chemical shifts typically observed for the equivalent methylene signals in the smaller trimer CTV, indicating that, at least on an NMR timescale, ligand **2** in $[Pd_4Cl_8(\mathbf{2})]$ adopts a "distorted-cup" conformation that is previously unobserved for CTTV. The distorted-cup conformation is intermediate between the C_4-symmetric "crown" conformation and the "boat" conformation. Further supporting this assertion, the signal for the aryl protons of the CTTC core move dramatically downfield to approximately 7.96 ppm (cf. $\delta = 6.29$ and 6.72 ppm). This result is consistent with the hydrogen atom being heavily deshielded by both the adjacent aryl rings of the CTTC core and the coordinated palladium(II) cations, which occurs within a distorted-cup conformation for the complex. Similar downfield shifts are observed for the OCH_2py signals of the ligand, which are located in a similar environment.

A VT NMR spectroscopic study on $[Pd_4Cl_8(\mathbf{2})]$ revealed no significant changes to the ^{1}H NMR spectrum on warming or cooling the sample (293–353 K). This indicated that the complex formed is conformationally locked in solution. Conformational locking of $[Pd_4Cl_8(\mathbf{2})]$ is only anticipated if the palladium atoms bridge between pyridyl rings on different veratrole units in **2**, as was the binding mode observed in the crystal structure of DMF⊂$[Pd_3Cl_6(\mathbf{1})]$·DMF. This binding mode also necessitates either a crown or distorted-cup conformation. The alternative and less likely arrangement of the complex, whereby chelation to the palladium(II) cations is by the pyridyl donors of each individual veratrole moiety, is likely to present a species with a boat or sofa conformation that rapidly converts in solution. Note that the $[Ag_4(\mathbf{2})]^{4+}$ complex shows the alternative ligand-binding mode and does exist in the boat conformation in the solid state, and in solution at room temperature appears to undergo slow interconversion of the equivalent boat conformations consistent with a broad ^{1}H NMR spectrum for the compound.

Calculations on $[Pd_4Cl_8(\mathbf{2})]$: In an attempt to better understand the conformation and ligand-binding mode of $[Pd_4Cl_8(\mathbf{2})]$, a series of density functional theory calculations was undertaken. The geometries of the complex in both a distorted-cup conformation, with palladium atoms bridged by pyridyl rings from different veratrole units, and a sofa conformation, with the palladium atoms bridged by pyridyl rings from the same veratrole units, were optimised. These calculations provide the energies of each structure and the distorted-cup conformation is more stable by approximately 90 kJ mol^{-1}. A snapshot of this calculated structure is given in Figure 5 and shows a distorted-cup conformation that possesses a cavity suitable for guest binding, somewhat like the crown conformation with its strict C_{4v} symmetry. From these data, the IR spectrum may be calculated and compared to the observed spectrum (Figure 6).

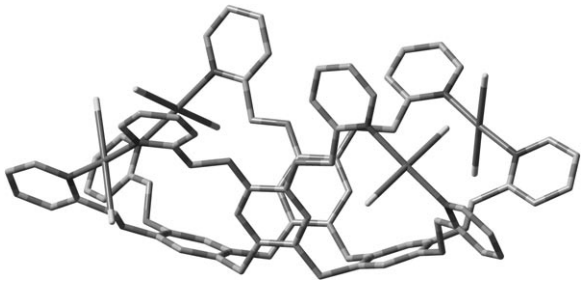

Figure 5. A view of the calculated structure of the conformation of $[Pd_4Cl_8(\mathbf{2})]$, which shows that the veratrole units are all pointing up to generate a "distorted-cup" conformation of the CTTC core.

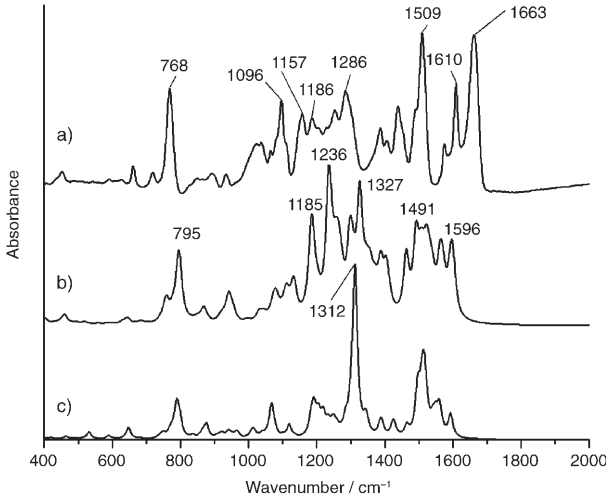

Figure 6. IR spectra of $[Pd_4Cl_8(\mathbf{2})]$: a) experimental IR (KBr disc); b) calculated "distorted-cup" form; c) calculated "sofa" form.

The experimental and simulated IR spectra are shown in Figure 6. The experimental data show strong bands at 768, 1509, 1610 and 1663 cm^{-1} with a group of features from 1157 to 1286 cm^{-1}. The simulated spectra are significantly different between the sofa and distorted-cup forms; the sofa form has a very strong predicted band at 1312 cm^{-1} with very weak transitions at lower wavenumbers. In the case of the distorted-cup form, a number of bands are predicted that correspond to the observed transitions between 1157 and 1286 cm^{-1}; these include the bands predicted at 1185, 1236 and 1327 cm^{-1}. In addition to these differences in the calculated spectra, the two conformers show a number of common bands at approximately 795, 1500 and 1596 cm^{-1}. These common bands are due to stretching and torsional modes of the peripheral pyridine units. The conformer distinct bands in the 1150 to 1350 cm^{-1} region are, however, associated with vibrational modes of the CTTC moiety. The normal modes for the sofa 1312 cm^{-1} band and the distorted-cup 1327 cm^{-1} band are shown in Figure 7. The IR data are consistent with the presence of a distorted-cup conformation in $[Pd_4Cl_8(\mathbf{2})]$ and the proposed cross-veratrole coordination mode.

The distorted-cup conformation postulated for $[Pd_4(\mathbf{2})Cl_8]$ suggests that this complex would make an ideal host for small organic molecules. However, the disposition of the coordinated chloride anions may preclude such a species from functioning as a host for larger guest molecules, such as carboranes and fullerenes. Nonetheless, during efforts to prepare crystals of $[Pd_4Cl_8(\mathbf{2})]$, co-crystallisations of the complex were attempted with a large range of small organic guests (as solvents) and larger guests, such as neutral carbaboranes. Unfortunately no crystals were obtained. Recently, a metallo-locked extended calix[4]arene derivative, capable of including cavitands within its own host cavity, was reported.[20] This species is conformationally locked by the metal centres akin to the palladium species described herein.

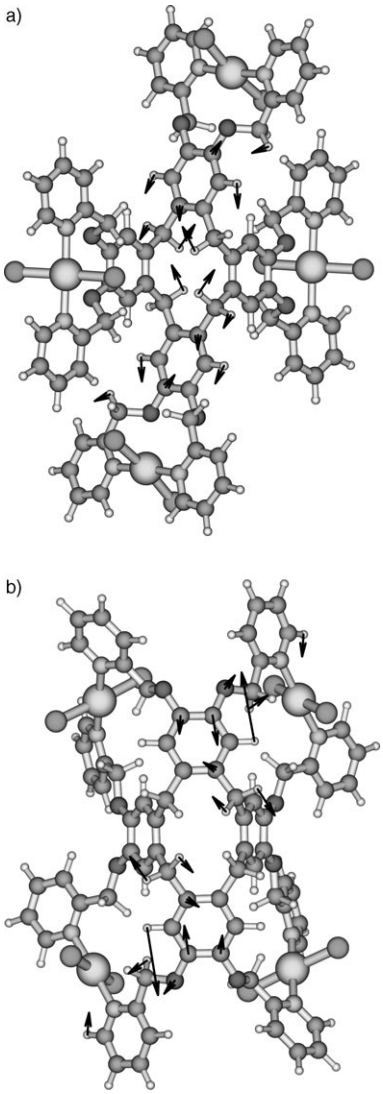

Figure 7. Normal modes associated with $[Pd_4Cl_8(\mathbf{2})]$: a) 1312 cm^{-1} band of the "sofa" form; b) 1327 cm^{-1} band of the "distorted-cup" form.

Structure of $[Ag_4(2)][Co(C_2B_9H_{11})_2]_4 \cdot 2.8\,CH_3CN \cdot H_2O$: The crystal structure of this complex represents the first solid-state structural evidence of the boat conformation of the CTTV motif. In the $[Ag_4(\mathbf{2})]^{4+}$ complex, the ligand adopts a boat conformation with two alternate veratrole moieties lying in a plane and the intervening two moieties perpendicular to those and mutually in plane (Figure 8). The adoption of this boat conformation appears to be stabilised by intra- and possibly intermolecular π-stacking interactions. In particular, there are intramolecular π-stacking interactions between the two veratrole units (benzene and pyridyl rings) that comprise the two sides of the boat. The ring centroid–centroid distances are 3.35 Å (veratrole rings), and 3.78 and 3.75 Å (pyridyl groups).[21] Despite appearances, silver–silver interactions do not appear to be significantly stabilising this boat structure.

The tetranuclear silver complex crystallises in the triclinic space group $P\bar{1}$ with one complete cation of the $[Ag_4(\mathbf{2})]^{4+}$ complex, four cobalticarborane anions, and three acetonitrile and one water solvate molecules in the asymmetric

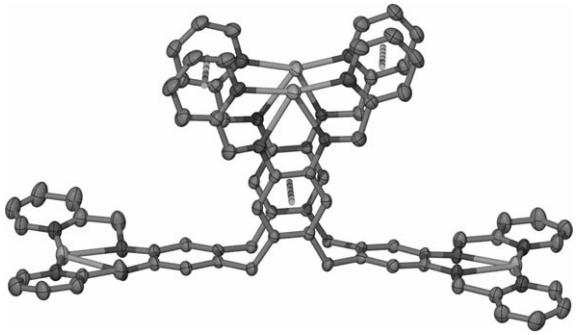

Figure 8. ORTEP representation (at the 50% probability level) of the cationic $[Ag_4(\mathbf{2})]^{4+}$ moiety of the crystal structure of $[Ag_4(\mathbf{2})][Co(C_2B_9H_{11})_2]_4 \cdot 2.8\,CH_3CN \cdot H_2O$. The intramolecular π-stacking interactions are shown with dashed bonds. Hydrogen atoms, solvate molecules and anions are omitted for clarity.

unit. The ligand chelates to four different silver atoms in the binding pockets initially proposed for this ligand. Each silver centre is coordinated by two pyridyl nitrogen atoms (Ag–N bond lengths: 2.158(4)–2.219(4) Å) and interacts with the ether oxygen linkers of the ligand to varying extents (Ag–O distances: 2.555(3)–2.793(3) Å). These bonding interactions result in a four-coordinate silver centre with a distorted planar geometry.[22] The silver cations are prevented from making any further bonds to solvate molecules by the adjacent, sterically demanding carborane anions (Figure 9); in one case, a weak 3c–2e interaction with an

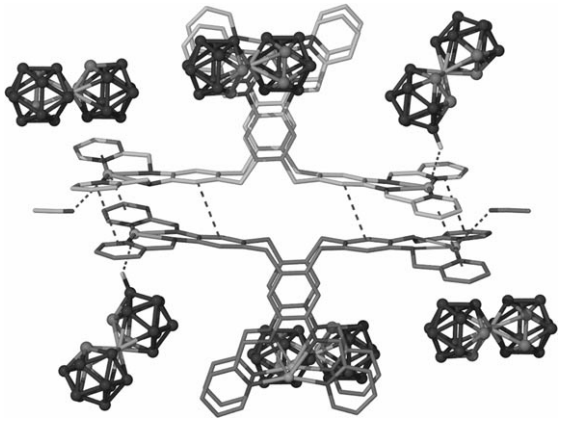

Figure 9. Perspective view of the local packing environment of the discrete complexes of $[Ag_4(\mathbf{2})]^{4+}$. The complexes form a dimeric assembly (weak π stacking indicated by dashed bonds) in which six of the silver cations are "capped" by cobalticarborane anions. One of these forms a long 3c–2e bond (dashed bond). An acetonitrile molecule packs into the cleft between the two $[Ag_4(\mathbf{2})]^{4+}$ complexes. Hydrogen atoms (except the hydrogen atoms involved in the 3c–2e bond), non-coordinated solvate molecules and remaining anions are omitted for clarity.

Ag1···H–B distance of 2.35 Å complements the coordinate bonds. This distance is slightly longer than other reported examples of Ag···H–B interactions with carbaborane anions that tend to be in the range 2.0–2.2 Å.[23] An acetonitrile solvate molecule also makes a weak interaction with Ag3 (Ag–N distance: 2.803(4) Å). The intramolecular distance between the two silver atoms located in the "sides" of the boat is 3.550(1) Å and thus well outside the range considered to represent Ag–Ag bonding interactions.[24]

Within the crystal structure, discrete complexes pack as dimers with intermolecular π-stacking interactions (centroid–centroid distances of 3.78–3.89 Å) between the two molecules.[21] The ring centroid–centroid distances are longer than the intramolecular values given above, which indicates that these intermolecular π-stacking interactions are weaker. The intermolecular silver–silver distances are too long to be considered bonding (3.582(1) Å), and thus π-stacking interactions and steric repulsions between the ligands govern the separation between the molecules in the dimeric motif (Figure 6). The packing is completed by association of these dimers into chains by π-stacking interactions (involving the veratrole moieties not capped by carbaborane anions), which in turn appear to be surrounded by a "coat" of cobalticarborane anions that isolate individual chains.

The boat conformation of the CTTV core has previously been observed in solution for dodecamethoxyorthocyclophane in polar solvents at room temperature in $[D_5]$nitrobenzene and for CTTV in acetonitrile at −40 °C.[13] Previously reported inclusion complexes of CTTV and CTTC showed that the host veratrylene has always adopted a sofa ("chair") conformation.[4–6,25] To our knowledge, this represents the first solid-state observation of the boat conformation. The boat conformation observed here may, in part, be an artefact of crystallisation, but importantly is favoured by the coordination of the four silver cations in the manner observed. This constrains the pyridyl groups and veratrole rings to which they are appended into the same plane, favours the π-stacking interactions and hence supports the observed boat conformation. The silver(I) cation is a better fit to the chelating veratrole sites of the ligand than a palladium(II) cation, as the silver(I) centre can accommodate slightly longer M–L bonds.

Conclusion

We have reported the synthesis of the new ligand **2**, which was demonstrated by a VT NMR spectroscopic investigation to adopt a sofa conformation. This conformation interconverts on the NMR timescale at elevated and room temperature. This is in distinct contrast to the chemistry of the related trimeric homologue **1**, which exists in a stable bowl conformation. Ligand **1** readily forms trinuclear complexes with silver(I), copper(II) and palladium(II). For palladium(II) chloride, crystal structures revealed the metal centres to lie in a position that bridged adjacent veratrole moieties, rather than chelating within a single veratrole subunit as initially expected.

The coordination chemistry of **2** revealed insights into possible ways to control the conformation mobility of CTTV derivatives. Whereas the free ligand adopts a sofa conformation in solution, the tetranuclear palladium complex of **2** adopts a distorted-cup conformation in solution at room temperature and this conformation is also stable across a large temperature range. Furthermore, when **2** was reacted with $Ag[Co(C_2B_9H_{11})_2]$, a tetranuclear silver complex was obtained that adopts a boat conformation in the solid state. Hence, we have demonstrated the sofa conformation for the free ligand **2**, the boat conformation in a silver complex of **2**, and a structure showing some features of the elusive crown conformation for $[Pd_4Cl_8(\mathbf{2})]$. This latter distorted-cup structure promises interesting possibilities in terms of host–guest chemistry.

Experimental Section

General experimental: IR spectra were measured for compounds as solid-state samples on a Perkin–Elmer FTIR spectrometer. The micro-

analytical laboratory at the University of Leeds performed elemental analyses, typically on samples that were dried in vacuo for several hours. ESMS were recorded by using Micromass LCT or Bruker MicroTOF Focus mass spectrometers. NMR spectra were recorded on a range of instruments including Bruker DPX 300- and Bruker Avance 500-MHz spectrometers by using 5 mm probes. The ^{1}H NMR spectra recorded were referenced relative to the internal standard Me_4Si, or to the solvent peak: [D$_6$]DMSO, $\delta = 2.6$ ppm. ^{13}C NMR spectra were all referenced to their solvent peaks: $CDCl_3$, $\delta = 77.0$ ppm; [D$_6$]DMSO, $\delta = 39.6$ ppm. VT NMR spectroscopic studies on [Pd_4Cl_8(**2**)] were conducted in [D$_6$]DMSO over a temperature range of 293–353 K and spectra were collected at 10 K increments. Unless otherwise stated, reagents were obtained from commercial sources and used as received. The following compounds were prepared by literature methods: CTTV,[26] CTTC[2,5,6] and **1**.[12]

Synthesis of 2

Method A: A suspension of CTTC (245 mg, 0.502 mmol), 2-bromomethylpyridine hydrobromide (1078 mg, 4.30 mmol), [18]crown-6 (105 mg, 0.40 mmol) and sodium carbonate (1.70 g, 12.3 mmol) was refluxed in acetone (60 mL) for 96 h under a nitrogen atmosphere. After cooling, the solvent was removed in vacuo and the solid extracted with dichloromethane (3×50 mL). The combined extracts were washed with water (50 mL), dried over magnesium sulfate and taken to dryness to give an oily solid. The solid was triturated with methanol, collected, washed with methanol then diethyl ether and dried under vacuum to give **2** (105 mg, 17%).

Method B: A suspension of CTTC (245 mg, 0.502 mmol), 2-chloromethylpyridine hydrochloride (701 mg, 4.27 mmol) and caesium carbonate (2.59 g, 7.96 mmol) was heated at 80 °C in DMF (10 mL) for 96 h under a nitrogen atmosphere. After cooling, water (100 mL) was added and the suspension extracted with dichloromethane (3×75 mL). The combined extracts were dried over sodium sulfate and taken to dryness to give an oily solid. The solid was triturated with methanol, collected, washed with methanol and dried under vacuum to give **2** (170 mg, 28%).

M.p. 229–232 °C; ^{1}H NMR (500 MHz, $CDCl_3$, Me_4Si, 233 K): $\delta = 2.92$ (d, $J = 15.9$ Hz, 4H; CH_2), 3.48 (d, $J = 15.9$ Hz, 4H; CH_2), 4.86 (d, $J = 13.6$ Hz, 4H; OCH_2), 4.97 (d, $J = 13.6$ Hz, 4H; OCH_2), 5.47 (s, 8H; OCH_2), 6.10 (s, 4H; aryl H), 6.60 (s, 4H; aryl H), 7.25 (m, 8H; H5, H5), 7.42 (d, $J = 7.8$ Hz, 4H; H3), 7.66 (t, $J = 7.6$ Hz, 4H; H4), 7.78 (d, $J = 7.9$ Hz, 4H; H3), 7.87 (t, $J = 7.6$ Hz, 4H; H4), 8.54 (d, $J = 4.4$ Hz, 4H; H6), 8.64 ppm (d, $J = 4.3$ Hz, 4H; H6); ^{1}H NMR (500 MHz, $CDCl_3$, Me_4Si, 303 K): $\delta = 3.00$ (brs, 4H; CH_2), 3.51 (brs, 4H; CH_2), 5.04 (brs, 8H; OCH_2py), 5.38 (brs, 8H; OCH_2py), 6.29 (brs, 4H; aryl CH), 6.72 (brs, 4H; aryl CH), 7.18 (s, 8H; pyH5), 7.70 (brm, 16H; pyH3/H4), 8.55 ppm (s, 8H; pyH6); ^{1}H NMR (500 MHz, $CDCl_3$, Me_4Si, 333 K): $\delta = 3.33$ (brs, 8H; CH_2), 5.15 (brs, 16H; OCH_2py), 6.53 (brs, 8H; aryl CH), 7.13 (dd, $J = 6.7$, 5.3 Hz, 8H; pyH5), 7.55 (brs, 8H; pyH3), 7.64 (t, $J = 6.8$ Hz, 8H; pyH4), 8.52 ppm (d, $J = 4.3$ Hz, 8H; pyH6); ^{13}C NMR (125.64 MHz, $CDCl_3$, Me_4Si, 333 K): $\delta = 34.74$, 72.39, 117.41, 121.44, 122.41, 132.54, 136.59, 147.15, 149.15, 157.97 ppm; ESMS: *m*/*z* (%): 1240.1 [*M*+Na]$^+$, 1217.1 (*M*$^+$); HRMS: *m*/*z*: calcd for $C_{76}H_{65}N_8O_8^+$: 1217.4920; found: 1217.4869; elemental analysis calcd (%) for $C_{76}H_{64}N_8O_8 \cdot H_2O$: C 73.9, H 5.4, N 9.1; found: C 73.5, H 5.25, N 8.7.

[Ag_3(1)][Co($C_2B_9H_{11}$)$_2$]$_3$: A solution of **1** (9.8 mg, 0.011 mmol) dissolved in dichloromethane was layered with methanol (1 mL) and then a methanolic solution of Ag[Co($C_2B_9H_{11}$)$_2$] (15.1 mg, 0.035 mmol) layered over the top. Following slow mixing of the layers, a yellow solid precipitated. Yield 9.5 mg (39%); ^{1}H NMR (500 MHz, CD_3CN, 303 K): $\delta = 3.57$ (d, $J = 14.3$ Hz, 3H; CH_2), 3.85 (brs, 12H; carbaborane CH), 4.71 (d, $J = 14.2$ Hz, 3H; CH_2), 5.25 (m, 12H; CH_2–O), 7.17 (s, 6H; aryl CH), 7.45 (t, $J = 6.7$ Hz, 6H; pyH5), 7.64 (d, $J = 7.8$ Hz, 6H; pyH3), 7.91 (t, $J = 7.6$ Hz, 6H; pyH4), 8.66 ppm (d, $J = 4.8$ Hz, 6H; pyH6); IR: $\tilde{\nu}_{max} = 3651$, 3040, 2922, 2864, 2511, 1605, 1573, 1509, 1488, 1442, 1403, 1390, 1338, 1306, 1270, 1224, 1190, 1158, 1141, 1095, 1058, 1018, 981, 944, 919, 885, 759, 723, 686, 643, 628, 617, 580, 535, 471 cm^{-1}; ESMS: *m*/*z* (%): 1452.5 ([Ag_2(**1**)][Co($C_2B_9H_{11}$)$_2$]$^+$), 1021.3 ([Ag(**1**)]$^+$), 913.4 (**1**$^+$), 779.7 ([Ag_3(**1**)][Co($C_2B_9H_{11}$)$_2$]$^{2+}$), 564.2 ([Ag_2(**1**)]$^{2+}$); elemental analysis calcd (%) for $C_{69}H_{114}B_{54}N_6O_6Co_3Ag_3$: C 37.5, H 5.2, N 3.8; found: C 38.4, H 4.9, N 3.7.

[Cu_3(1)Cl_6]·H_2O: $CuCl_2 \cdot 2H_2O$ (6.8 mg, 0.040 mmol) and **1** (10.0 mg, 0.011 mmol) were mixed together in DMF (ca. 1 mL) and heated at 100 °C for 60 min. During this time a pale-blue precipitate formed that was collected by filtration, washed with methanol then diethyl ether, and dried under vacuum. Yield 6.4 mg (44%); IR: $\tilde{\nu}_{max} = 3540$, 3072, 2923, 1641, 1610, 1573, 1515, 1481, 1447, 1401, 1340, 1278, 1231, 1190, 1140, 1092, 1049, 1029, 945, 883, 837, 767, 729, 691, 648, 640, 631, 605, 536, 487 cm^{-1}; elemental analysis calcd (%) for $C_{57}H_{48}N_6O_6Cl_6Cu_3 \cdot H_2O$: C 51.3, H 3.8, N 6.3; found: C 51.3, H 4.15, N 6.4.

[Cu_3(1)Br_6]: $CuBr_2$ (8.8 mg, 0.039 mmol) and **1** (10.5 mg, 0.011 mmol) were mixed together in DMF (ca. 1 mL) and heated at 100 °C for 60 min. During this time a khaki-green precipitate formed that was collected by filtration, washed with methanol then diethyl ether, and dried under vacuum. Yield 7.7 mg (44%); IR: $\tilde{\nu}_{max} = 3544$, 3074, 3031, 2919, 1667, 1608, 1574, 1511, 1493, 1477, 1447, 1392, 1347, 1318, 1298, 1273, 1228, 1190, 1154, 1098, 1057, 1028, 944, 933, 883, 835, 766, 725, 660, 648, 637, 607, 536, 487 cm^{-1}; elemental analysis calcd (%) for $C_{57}H_{48}N_6O_6Br_6Cu_3$: C 43.2, H 3.1, N 5.3; found: C 43.3, H 3.3, N 5.55.

[Pd_3(1)Cl_6]·solvent

Method A: A solution of $Na_2[PdCl_4]$ (10.4 mg, 0.035 mmol) in methanol was layered over a dichloromethane solution of **1** (10.8 mg, 0.012 mmol). After standing overnight, small yellow crystals with a needle-like morphology formed in the vial. Removal of the crystals from the mother liquor resulted in rapid loss of solvent, preventing characterisation by X-ray crystallography. Yield 6.3 mg (40%); sample contaminated with sodium chloride. Elemental analysis calcd (%) for $C_{57}H_{48}N_6O_6Cl_6Pd_3$: C 47.4, H 3.35, N 5.8; calcd for $C_{57}H_{48}N_6O_6Cl_6Pd_3 \cdot 2NaCl$: C 43.8, H 3.1, N 5.4; found: C 44.1, H 3.15, N 4.9.

Method B: $Na_2[PdCl_4]$ (20.4 mg, 0.069 mmol) and **1** (20.0 mg, 0.022 mmol) were mixed together in DMF (3 mL) and heated at 100 °C for 60 min. This gave a moderate amount of a crystalline yellow solid that contained crystals suitable for X-ray crystallography. This crystalline solid was collected by filtration, washed with small quantities of hot water (to remove precipitated NaCl), methanol, and then diethyl ether. The solid was finally dried. Yield 14.8 mg (42%); IR: $\tilde{\nu}_{max} = 3454$, 3079, 2921, 1667, 1608, 1575, 1515, 1493, 1440, 1386, 1346, 1270, 1216, 1190, 1143, 1092, 1064, 1025, 942, 883, 833, 764, 721, 660, 636, 607, 536, 485 cm^{-1}; elemental analysis calcd (%) for $C_{57}H_{48}N_6O_6Cl_6Pd_3 \cdot 2DMF$: C 47.6, H 3.94, N 7.04; found: C 46.2, H 4.15, N 7.4 (analysis carried out on a sample of crystals formed in the reaction). Additionally, the filtrate could be used to grow crystals of [Pd_2Cl_4 (**1**)] by vapour diffusion of ethanol into the filtrate over a period approximately two months. Small orange petal-shaped crystals formed in minuscule yield, which were suitable for crystallography although too poorly diffracting to yield a publishable structure.

Method C: $Na_2[PdCl_4]$ (20.6 mg, 0.070 mmol) and **1** (19.8 mg, 0.022 mmol) were mixed together in DMSO (2 mL) and heated at 100 °C for 60 min. This gave an orange solution from which a moderate amount of yellow solid precipitated. This solid was collected by filtration, washed with a small quantity of water, methanol, and diethyl ether, and the resulting solid was then dried. Yield 13.0 mg (39%); IR: $\tilde{\nu}_{max} = 3402$, 3082, 2910, 1661, 1608, 1575, 1519, 1493, 1436, 1403, 1386, 1346, 1270, 1216, 1190, 1143, 1090, 1139, 1091, 1060, 1025, 951, 884, 847, 833, 764, 720, 660, 636, 608, 536, 485 cm^{-1}; elemental analysis calcd (%) for $C_{57}H_{48}N_6O_6Cl_6Pd_3 \cdot 2DMSO$: C 45.8, H 3.8, N 5.25; found: C 45.9, H 4.0, N 5.45. The precipitates and crystals obtained in the above reactions were insoluble in common laboratory NMR solvents, and therefore no characterisation was undertaken in solution by NMR spectroscopy.

[Pd_3(CF_3COO)$_6$ (1)]: A yellow solution of Pd(CF_3COO)$_2$ (11.8 mg, 0.035 mmol) in methanol was mixed with a dichloromethane solution of **1** (10.2 mg, 0.011 mmol). After standing for several days, small yellow crystals formed within a black precipitate (Pd metal). Separation and collection of the yellow crystals was achieved by decanting the solution and black precipitate. The crystals were washed with methanol followed by diethyl ether, and then dried in vacuo. Removal of the crystals from the mother liquor resulted in extremely rapid decomposition consistent with loss of solvent. Yield 3.2 mg (15%). IR: $\tilde{\nu}_{max} = 3122$, 3064, 2937, 1685, 1610, 1577, 1509, 1493, 1446, 1403, 1379, 1282, 1182, 1154, 1089, 1068,

1039, 1010, 966, 946, 899, 870, 852, 790, 773, 733, 661, 629, 573, 523, 485 cm^{-1}; elemental analysis calcd (%) for $C_{69}H_{48}N_6O_{18}F_{18}Pd_3$: C 43.4, H 2.5, N 4.4; found: C 43.1, H 2.1, N 3.8.

$[Ag_4(2)][Co(C_2B_9H_{11})_2]_4 \cdot 2.8\,CH_3CN \cdot H_2O$: A solution of **2** (20.1 mg, 0.016 mmol) dissolved in dichloromethane was mixed with an acetonitrile solution of $Ag[Co(C_2B_9H_{11})_2]$ (28.6 mg, 0.066 mmol). Slow evaporation of the reaction mixture gave yellow crystals. Yield 22.0 mg (45%); IR: $\tilde{\nu}_{max}$ = 3413, 3038, 2924, 2532 (BH stretch), 1604, 1572, 1512, 1449, 1407, 1389, 1364, 1279, 1226, 1193, 1149, 1096, 1016, 981, 883, 760, 722, 686, 620, 558, 478 cm^{-1}; ESMS: *m/z*: no peaks corresponding to the expected molecular ion; elemental analysis calcd (%) for $C_{97.6}H_{162.4}B_{72}N_{10.8}O_9Co_4Ag_4$: C 38.2, H 5.3, N 5.0; found: C 41.9, 41.9; H 5.15, 5.15; N 4.8, 4.5.

$[Cu_4(2)Br_8]$: $CuBr_2$ (14.9 mg, 0.0168 mmol) and **2** (20.5 mg, 0.067 mmol) were mixed together in DMF (ca. 2 mL) and heated at 100°C for 60 min. During this time a khaki-green precipitate formed that was collected by filtration, washed with methanol and dichloromethane, and dried under vacuum. Yield 18 mg (51%); IR: $\tilde{\nu}_{max}$ = 3468, 3065, 3035, 2900, 2865, 1673, 1609, 1574, 1514, 1446, 1409, 1392, 1359, 1285, 1251, 1228, 1193, 1159, 1102, 1050, 1029, 939, 891, 852, 833, 788, 767, 727, 646, 632, 593, 553, 534, 517, 495 cm^{-1}; elemental analysis calcd (%) for $C_{76}H_{64}N_8O_8Br_8Cu_4$: C 43.2, H 3.1, N 5.3; found: C 42.6, H 3.05, N 5.15.

$[Pd_4Cl_8(2)] \cdot 4H_2O$

Method A: A filtered methanol solution of $Na_2[PdCl_4]$ (51.3 mg, 0.174 mmol) was added dropwise to a stirred solution of **2** (50.3 mg, 0.041 mmol) in dichloromethane (10 mL). A fine yellow precipitate formed immediately and the suspension was stirred for 10 min. The solid was collected by filtration and washed with a small quantity of DMSO, methanol, dichloromethane, and finally diethyl ether before drying under vacuum. A second crop was obtained from the washings. Yield 67 mg (82%); ^{1}H NMR (500 MHz, [D$_6$]DMSO, 303 K): δ = 4.04 (d, *J* = 14.5 Hz, 4H; CH_2), 4.87 (d, *J* = 14.4 Hz 4H; CH_2), 6.12 (d, *J* = 14.0 Hz, 8H; OCH_2py), 6.27 (d, *J* = 14.2 Hz 8H; OCH_2py), 7.70 (t, *J* = 6.7 Hz, 8H; pyH5), 7.96 (s, 8H; aryl CH), 8.00 (d, *J* = 7.7 Hz 8H; pyH3), 8.26 (t, *J* = 8.1 Hz, 8H; pyH4), 9.42 ppm (d, *J* = 5.2 Hz, 8H; pyH6); IR: $\tilde{\nu}_{max}$ = 3522, 3077, 2962, 1608, 1573, 1505, 1441, 1404, 1378, 1284, 1228, 1186, 1160, 1098, 1065, 1033, 935, 895, 823, 768, 718, 658, 630, 502, 455 cm^{-1}; ESMS: *m/z* (%): 927.5 ([Pd$_4$ Cl$_6$ (**2**)]$^{2+}$); elemental analysis calcd (%) for $C_{76}H_{64}N_8O_8Cl_8Pd_4 \cdot 4H_2O$: C 45.7, H 3.6, N 5.6; found: C 45.6, H 3.55, N 5.5.

Method B: $Na_2[PdCl_4]$ (19.9 mg, 0.068 mmol) and **2** (19.8 mg, 0.016 mmol) were mixed together in DMF (3 mL) and heated at 80°C for 60 min. A small amount of a precipitate was removed by filtration and then vapour diffusion of methanol into the filtrate of the reaction mixture yielded a yellow solid. Yield 16.0 mg (50%); IR: $\tilde{\nu}_{max}$ = 3438, 3080, 2919, 2849, 1707 (C=O stretch), 1664, 1609, 1576, 1514, 1439, 1402, 1362, 1261, 1220, 1195, 1151, 1090, 1024, 937, 881, 848, 769, 720, 660, 627, 591, 557, 530, 454 cm^{-1}; elemental analysis calcd (%) for $C_{76}H_{64}N_8O_8Cl_8Pd_4 \cdot 4H_2O$: C 45.7, H 3.6, N 5.6; found: C 45.5, H 3.4, N 5.45.

Method C: $Na_2[PdCl_4]$ (19.2 mg, 0.065 mmol) and **2** (19.9 mg, 0.016 mmol) were mixed together in DMSO (3 mL) and heated at 80°C for 60 min. This gave an orange solution from which a moderate amount of solid precipitated. Vapour diffusion of methanol into the filtrate of the reaction mixture yielded a yellow solid. Yield 10.8 mg (34%); $\tilde{\nu}_{max}$ = 3524, 3080, 2911, 1609, 1575, 1513, 1440, 1402, 1377, 1284, 1197, 1152, 1095, 1123, 937, 846, 766, 719, 660, 622, 557 cm^{-1}; elemental analysis calcd (%) for $C_{76}H_{64}N_8O_8Cl_8Pd_4 \cdot 4H_2O$: C 45.7, H 3.6, N 5.6; found: C 45.7, H 3.4, N 5.25.

X-ray crystallography: Crystals were mounted under oil or grease onto a glass fibre and X-ray data were collected at low temperatures with $Mo_{K\alpha}$ radiation (λ = 0.71073 Å) on either a Nonius Kappa CCD diffractometer or a Bruker Nonius X8 diffractometer fitted with an Apex II detector and FR591 rotating anode operating at 4 kW. Data sets were corrected for absorption by using a multiscan method.[27] Structures were typically solved by direct methods by using SHELXS-97[28] and refined by full-matrix least-squares on F^2 by SHELXL-97,[29] interfaced through the program X-Seed.[30] In general, all non-hydrogen atoms were refined anisotropically and hydrogen atoms were included as invariants at geometrically estimated positions. Deviations from this procedure are described with specific structures in the section that follows. Diagrams were generated by using the program X-Seed[30] as an interface to POV-Ray.[31] CCDC-669036, 669037 and 669038 contain the supplementary crystallographic data for this paper. These data can be obtained free of charge from The Cambridge Crystallographic Data Centre via www.ccdc.cam.ac.uk/data_request/cif.

Crystal data for DMF⊂$[Pd_3Cl_6(1)]$·DMF: $C_{63}H_{62}Cl_6N_8O_8Pd_3$; F_W = 1591.11; monoclinic; $P2_1/m$; *a* = 10.4340(6), *b* = 19.342(1), *c* = 17.0617(9) Å; β = 100.733(3)°; *V* = 3383.0(3) Å^3; *Z* = 2; ρ = 1.562 mg cm^{-3}; μ = 1.084 mm^{-1}; *F*(000) = 1600; yellow plate; 0.26 × 0.11 × 0.03 mm; $2\theta_{max}$ = 56.94°; *T* = 150(2) K; 36190 reflections, 8714 unique (99.2% completeness); R_{int} = 0.0344; 427 parameters; GOF = 1.048; *wR*2 = 0.2998 for all data; R_1 = 0.0854 for 5022 data with $I > 2\sigma(I)$.

Additional crystallographic information: The largest peak (2.68 e Å^3) in the Fourier difference map is located 0.90 Å from one of the Pd atoms. Other peaks are located around the Cl atoms of the structure. The bond lengths of the lattice including the DMF molecule, which is disordered across the mirror plane with symmetry-imposed 50% occupancy of both sites, were restrained with DFIX commands generating three restraints.

Crystal data for $(DMF)_{0.5}$⊂$[Pd_2Cl_4(1)] \cdot 2H_2O$: $C_{58.5}H_{59.5}Cl_4N_{6.5}O_{8.5}Pd_2$; F_W = 1344.23; orthorhombic; *Pnma*; *a* = 20.8290(4), *b* = 22.1910(5) *c* = 26.5780(7) Å; *V* = 12284.8(5) Å^3; *Z* = 8; ρ = 1.454 mg cm^{-3}; μ = 0.817 mm^{-1}; *F*(000) = 5472; yellow petal-shaped plate; 0.23 × 0.12 × 0.05 mm; $2\theta_{max}$ = 50.12°; *T* = 150(2) K; 57204 reflections, 11125 unique (99.3% completeness); R_{int} = 0.0882; 634 parameters; GOF = 1.030; *wR*2 = 0.3080 for all data, R_1 = 0.0896 for 6775 data with $I > 2\sigma(I)$.

Additional crystallographic information: The unbound pyridyl groups showed significant disorder and were each refined over two positions with rigid body refinement (AFIX 66) and occupancies set to rounded refined values. Atoms in the unbound pyridyl groups were refined with isotropic displacement parameters. The residual electron density was too diffuse to adequately model all solvent molecules.

Crystal data for $[Ag_4(2)][Co(C_2B_9H_{11})_2]_4 \cdot 2.8\,CH_3CN \cdot H_2O$: $C_{97.6}H_{162.4}Ag_4B_{72}Co_4N_{10.8}O_9$; F_W = 3076.71; triclinic; $P\bar{1}$, *a* = 18.5966(2), *b* = 19.0694(2), *c* = 20.8202(3) Å; α = 91.3293(5), β = 108.7731(5), γ = 95.2327(5)°; *V* = 6950.6(2) Å^3; *Z* = 2; ρ = 1.470 mg cm^{-3}; μ = 1.073 mm^{-1}; *F*(000) = 3103; yellow plate; 0.20 × 0.16 × 0.04 mm; $2\theta_{max}$ = 54.96°; *T* = 150(1) K; 128345 reflections, 31670 unique (99.5% completeness); R_{int} = 0.0725; 1771 parameters; GOF = 1.018; *wR*2 = 0.1842 for all data, R_1 = 0.0615 for 20968 data with $I > 2\sigma(I)$.

Additional crystallographic information: The hydrogen atoms on the solvate water molecule could not be located in the Fourier difference map; one CH_3CN molecule was refined at 80% occupancy and with isotropic displacement parameters. The largest q peaks in the Fourier difference map are located around Co1A and the largest shifts in the refinement are associated with methyl hydrogen atoms of a CH_3CN solvent molecule.

Calculations: Density functional theory calculations were implemented by using the Gaussian suite of programs (G03W, C02 revision).[32] The B3LYP method was used for geometry and frequency calculations with a 6-31G(d) basis set for all atoms except Pd which were described by the LANL2DZ ECP.

Acknowledgement

The authors would like to acknowledge the support of the EPSRC in funding this research.

[1] J. D. White, B. D. Gesner, *Tetrahedron Lett.* **1968**, *13*, 1591–1594.
[2] J. D. White, B. D. Gesner, *Tetrahedron* **1974**, *30*, 2273–2277.

[3] a) M. J. Hardie, P. J. Nichols, C. L. Raston, *Adv. Supramol. Chem.* **2002**, *8*, 1–41; b) V. Percec, C. G. Cho, C. Pugh, *Macromolecules* **1991**, *24*, 3227–3234.
[4] a) M. Martinez, F. Lara Ochoa, R. Cruz-Almanza, R. A. Toscano, *J. Chem. Crystallogr.* **1996**, *26*, 451–456; b) H. Zhang, J. W. Steed, J. L. Atwood, *Supramol. Chem.* **1994**, *4*, 185–190.
[5] L. J. Barbour, J. W. Steed, J. L. Atwood, *J. Chem. Soc. Perkin Trans. 2* **1995**, 857–860.
[6] M. Martinez Garcia, P. Arroyo Ortega, F. Lara Ochoa, G. Espinosa Perez, S. Hernandez Ortega, M. I. Chavez Uribe, M. Salmon, R. Cruz-Almanza, *Tetrahedron* **1997**, *53*, 17633–17642.
[7] A. S. Lindsey, *J. Chem. Soc.* **1965**, 1685–1692.
[8] A. Collet, J. Gabard, *J. Org. Chem.* **1980**, *45*, 5400–5401.
[9] The alternative saddle conformation has recently been isolated by the rapid quenching of a hot solution or melt, see: H. Zimmermann, P. Tolstoy, H.-H. Limbach, R. Poupko, Z. Luz, *J. Phys. Chem. B* **2004**, *108*, 18772–18778, or within a CTV-based cryptophane, see S. T. Mough, J. C. Goeltz, K. T. Holman, *Angew. Chem.* **2004**, *116*, 5749–5753; *Angew. Chem. Int. Ed.* **2004**, *43*, 5631–5635.
[10] M. J. Hardie, C. L. Raston, *Chem. Commun.* **1999**, 1153–1163.
[11] a) M. J. Hardie, R. Ahmad, C. J. Sumby, *New J. Chem.* **2005**, *29*, 1231–1240; b) C. J. Sumby, J. Fisher, T. J. Prior, M. J. Hardie, *Chem. Eur. J.* **2006**, *12*, 2945–2959; c) M. J. Hardie, C. J. Sumby, *Inorg. Chem.* **2004**, *43*, 6872–6874; d) C. J. Sumby, M. J. Hardie, *Cryst. Growth Des.* **2005**, *5*, 1321–1324.
[12] M. J. Hardie, R. M. Mills, C. J. Sumby, *Org. Biomol. Chem.* **2004**, *2*, 2958–2964.
[13] a) A. Maliniak, Z. Luz, R. Poupko, C. Krieger, H. Zimmermann, *J. Am. Chem. Soc.* **1990**, *112*, 4277–4283; b) R. Lunkwitz, C. Tschierske, S. Diele, *J. Mater. Chem.* **1997**, *7*, 2001–2011; c) V. Percec, C. G. Cho, C. Pugh, *J. Mater. Chem.* **1991**, *1*, 217–222.
[14] a) J. A. Wytko, J. Weiss, *J. Inclusion Phenom. Mol. Recognit. Chem.* **1994**, *19*, 207–225; b) J. A. Wytko, C. Boudon, J. Weiss, M. Gross, *Inorg. Chem.* **1996**, *35*, 4469–4477; c) D. S. Bohle, D. J. Stasko, *Inorg. Chem.* **2000**, *39*, 5768–5770; d) D. S. Bohle, D. J. Stasko, *Chem. Commun.* **1998**, 567–568.
[15] a) D. A. McMorran, P. J. Steel, *Tetrahedron* **2003**, *59*, 3701–3707; b) A. M. Guerrero, F. A. Jalon, B. R. Manzano, R. M. Claramunt, M. D. Santa Maria, C. Escolastico, J. Elguero, A. M. Rodriguez, M. A. Maestro, J. Mahia, *Eur. J. Inorg. Chem.* **2002**, *12*, 3178–3189.
[16] M. R. A. Al-Mandhary, C. M. Fitchett, P. J. Steel, *Aust. J. Chem.* **2006**, *59*, 307–314.
[17] a) P. J. Steel, *Molecules*, **2004**, *9*, 440–448; b) P. J. Steel, *Acc. Chem. Res.* **2005**, *38*, 243–250.
[18] a) Y. J. Zhao, M. C. Hong, Y. C. Liang, W. P. Su, R. Cao, Z. Y. Zhou, A. S. C. Chan, *Polyhedron* **2001**, *20*, 2619–2625; b) P. Singh, S. Kumar, *Tetrahedron* **2006**, *62*, 6379–6387; c) P. Singh, S. Kumar, *Tetrahedron Lett.* **2006**, *47*, 109–112; d) C.-Y. Su, S. Liao, M. Wanner, J. Fiedler, C. Zhang, B.-S. Kang, W. Kaim, *Dalton Trans.* **2003**, 189–202; e) S. Tavacoli, T. A. Miller, R. L. Paul, J. C. Jeffery, M. D. Ward, *Polyhedron* **2003**, *22*, 507–514; f) R.-H. Wang, M.-C. Hong, W.-P. Su, Y.-C. Liang, R. Cao, Y.-J. Zhao, J.-B. Weng, *Bull. Chem. Soc. Jpn.* **2002**, *75*, 725–730; g) L. Sen, C.-Y. Su, Z.-F. Zhang, H.-Q. Liu, H.-L. Zhu, *Acta Cryst.* **2000**, *C56*, E348–E349; h) Y. Zhao, M. Hong, W. Su, R. Cao, Z. Zhou, A. S. C. Chan, *Chem. Lett.* **2000**, 28–29.
[19] a) D. A. McMorran, C. M. Hartshorn, P. J. Steel, *Polyhedron* **2004**, *23*, 1055–1061; b) C. M. Hartshorn, P. J. Steel, *J. Chem. Soc. Dalton Trans.* **1998**, 3935–3940; c) R. Peng, D. Li, T. Wu, X.-P. Zhou, S. W. Ng, *Inorg. Chem.* **2006**, *45*, 4035–4046; d) M. R. A. Al-Mandhary, P. J. Steel, *Eur. J. Inorg. Chem.* **2004**, 329–334.
[20] E. Botana, E. Da Silva, J. Benet-Buchholz, P. Ballester, J. de Mendoza, *Angew. Chem.* **2007**, *119*, 202–205; *Angew. Chem. Int. Ed.* **2007**, *46*, 198–201.
[21] C. Janiak, *J. Chem. Soc. Dalton Trans.* **2000**, 3885–3896.
[22] a) M. Munakata, L. P. Wu, T. Kuroda-Sowa, *Adv. Inorg. Chem.* **1999**, *46*, 174–304; b) A. N. Khlobystov, A. J. Blake, N. R. Champness, D. A. Lemenovskii, A. G. Majouga, N. V. Zyk, M. Schroder, *Coord. Chem. Rev.* **2001**, *222*, 155–192.
[23] a) K. Shelly, D. C. Finster, Y. J. Lee, W. R. Scheidt, C. A. Reed, *J. Am. Chem. Soc.* **1985**, *107*, 5955–5959; b) L. Cunha-Silva, R. Ahmad, M. J. Hardie, *Aust. J. Chem.* **2006**, *59*, 40–48; c) A. Westcott, N. Whitford, M. J. Hardie, *Inorg. Chem.* **2004**, *43*, 3663–3672.
[24] P. Pyykko, *Chem. Rev.* **1997**, *97*, 597–636.
[25] J. A. Hyatt, E. N. Duesler, D. Y. Curtin, I. C. Paul, *J. Org. Chem.* **1980**, *45*, 5074–5079.
[26] E. Al-Farhan, P. M. Keehn, R. Stevenson, *Tetrahedron Lett.* **1992**, *33*, 3591–3594.
[27] a) R. H. Blessing, *Acta Cryst.* **1995**, *A51*, 33–38; b) R. H. Blessing, *J. Appl. Crystallogr.* **1997**, *30*, 421–426.
[28] G. M. Sheldrick, *Acta Crystallogr.* **1990**, *A46*, 467–473.
[29] G. M. Sheldrick, *SHELXL-97*, University of Göttingen, Göttingen (Germany), **1997**.
[30] L. J. Barbour, *Supramol. Chem.* **2003**, *1*, 189–191.
[31] Persistence of Vision Raytracer Pty. Ltd., *POVRAY v. 3.5*, Williamstown, Victoria (Australia), **2002**.
[32] Gaussian 03, Revision C.02, M. J. Frisch, G. W. Trucks, H. B. Schlegel, G. E. Scuseria, M. A. Robb, J. R. Cheeseman, J. A. Montgomery, Jr., T. Vreven, K. N. Kudin, J. C. Burant, J. M. Millam, S. S. Iyengar, J. Tomasi, V. Barone, B. Mennucci, M. Cossi, G. Scalmani, N. Rega, G. A. Petersson, H. Nakatsuji, M. Hada, M. Ehara, K. Toyota, R. Fukuda, J. Hasegawa, M. Ishida, T. Nakajima, Y. Honda, O. Kitao, H. Nakai, M. Klene, X. Li, J. E. Knox, H. P. Hratchian, J. B. Cross, C. Adamo, J. Jaramillo, R. Gomperts, R. E. Stratmann, O. Yazyev, A. J. Austin, R. Cammi, C. Pomelli, J. W. Ochterski, P. Y. Ayala, K. Morokuma, G. A. Voth, P. Salvador, J. J. Dannenberg, V. G. Zakrzewski, S. Dapprich, A. D. Daniels, M. C. Strain, O. Farkas, D. K. Malick, A. D. Rabuck, K. Raghavachari, J. B. Foresman, J. V. Ortiz, Q. Cui, A. G. Baboul, S. Clifford, J. Cioslowski, B. B. Stefanov, G. Liu, A. Liashenko, P. Piskorz, I. Komaromi, R. L. Martin, D. J. Fox, T. Keith, M. A. Al-Laham, C. Y. Peng, A. Nanayakkara, M. Challacombe, P. M. W. Gill, B. Johnson, W. Chen, M. W. Wong, C. Gonzalez, J. A. Pople, Gaussian Inc., Pittsburgh, PA, **2003**.

Received: November 30, 2007
Revised: February 11, 2008
Published online: March 26, 2008

